



Diel variation of mercury stable isotope ratios record photoreduction of PM_{2.5}-bound mercury

Qiang Huang^{1,2}, Jiubin Chen^{1,3,*}, Weilin Huang⁴, John R. Reinfelder⁴, Pingqing Fu⁵, Shengliu

5 Yuan¹, Zhongwei Wang¹, Wei Yuan¹, Hongming Cai¹, Hong Ren⁵, Yele Sun⁵ and Li He⁶

¹ SKLEG, Institute of Geochemistry, CAS, Guiyang 550081, China

² SKLOG, Guangzhou Institute of Geochemistry, CAS, Guangzhou 510640, China

³ Institute of Surface-Earth System Science, Tianjin University, 300072, China

⁴ Department of Environmental Sciences, Rutgers, The State University of New Jersey, New

10 Brunswick, NJ 08901, USA

⁵ LAPC, Institute of Atmospheric Physics, CAS, Beijing 100029, China

⁶ Laboratory of Hebei Institute of Regional Geology and Mineral Resources Survey,

Shijiazhuang 065000, China

*Corresponding author.

15 E-mail: jbchen@tju.edu.cn



Abstract. Mercury (Hg) bound to fine aerosols (PM_{2.5}-Hg) may undergo photochemical reaction that causes isotopic fractionation and obscures the initial isotopic signatures. In this study, we quantified Hg isotopic compositions for 56 PM_{2.5} samples collected between Sept. 15th and Oct. 16th, 2015 from Beijing, China, among which 26 were collected during the daytime (between 8:00 a.m. and 6:30 p.m.) and 30 during night (between 7:00 p.m. and 7:30 a.m.). The results show that diel variation was statistically significant ($p < 0.05$) for Hg content, $\Delta^{199}\text{Hg}$ and $\Delta^{200}\text{Hg}$, with Hg content during the daytime ($0.32 \pm 0.14 \mu\text{g g}^{-1}$) lower than at night ($0.48 \pm 0.24 \mu\text{g g}^{-1}$) and $\Delta^{199}\text{Hg}$ and $\Delta^{200}\text{Hg}$ values during the daytime (mean of $0.26\text{\textperthousand} \pm 0.40\text{\textperthousand}$ and $0.09\text{\textperthousand} \pm 0.06\text{\textperthousand}$, respectively) higher than during the nighttime ($0.04\text{\textperthousand} \pm 0.22\text{\textperthousand}$ and $0.06\text{\textperthousand} \pm 0.05\text{\textperthousand}$, respectively), whereas PM_{2.5} concentrations and $\delta^{202}\text{Hg}$ values showed insignificant ($p > 0.05$) diel variation. Geochemical characteristics of the samples and the air mass backward trajectories (PM_{2.5} source related) suggest that diel variation in $\Delta^{199}\text{Hg}$ values resulted primarily from the photochemical reduction of divalent PM_{2.5}-Hg, rather than variations in emission sources. The importance of photoreduction is supported by the strong correlations between $\Delta^{199}\text{Hg}$ and: (i) $\Delta^{201}\text{Hg}$ (positive, slope = 1.1), (ii) $\delta^{202}\text{Hg}$ (positive, slope = 1.15), (iii) content of Hg in PM_{2.5} (negative), (iv) sunshine durations (positive), and (v) ozone concentration (positive) observed for consecutive day-night paired samples. Our results provide isotopic evidence that local, daily photochemical reduction of divalent Hg is of critical importance to the fate of PM_{2.5}-Hg in urban atmospheres and that, in addition to variation in sources, photochemical reduction appears to be an important process that affects both the particle mass-specific abundance and isotopic composition of PM_{2.5}-Hg.

Keywords: Mass-independent fractionation; Atmospheric particulate mercury; Transport and transformation; Isotopic evidence of photoreduction



1 Introduction

40 Atmospheric mercury (Hg) consists of three operationally-defined forms including particle-bound Hg (PBM), gaseous oxidized Hg (GOM), and gaseous elemental Hg (GEM) (Selin, 2009). GEM is the most abundant (about 90%) and chemically stable form (Selin, 2009), and is transported at regional and global scales. GOM has short residence times as it can readily be dissolved in rain droplets, adsorbed on particulate matter (PM), and it reacts rapidly within both 45 gaseous and aqueous phases with or without PM. PBM contains mainly reactive Hg species such as Hg^{2+} and perhaps trace quantities of Hg^0 , and is transported at regional or local scales thereby reflecting Hg pollution and cycling within short distances from emission source (Selin, 2009; Subir et al., 2012). PBM has multiple sources and undergoes complex transport and transformation processes in the atmosphere (Subir et al., 2012).

50 This study aimed at characterizing the isotope compositions of $\text{PM}_{2.5}$ -Hg (particulate matter with aerodynamic diameter less than 2.5 micrometers) to better understand the complex transformation processes of PBM. Hg has seven stable isotopes and is known to exhibit both mass-dependent (MDF, represented by $\delta^{202}\text{Hg}$) and mass-independent (MIF, including odd-mass-number isotopic MIF (odd-MIF) and even-mass-number isotopic MIF (even-MIF), 55 represented by $\Delta^{199}\text{Hg}$, $\Delta^{201}\text{Hg}$, $\Delta^{200}\text{Hg}$ and $\Delta^{204}\text{Hg}$) fractionation during Hg transformations under various environmental conditions (Hintelmann and Lu, 2003; Jackson et al., 2004; Bergquist and Blum, 2007; Jackson et al., 2008; Gratz et al., 2010; Chen et al., 2012; Sherman et al., 2012). Prior studies have shown that MDF can be induced by several Hg transformation and transport processes (Bergquist and Blum, 2007; Kritee et al., 2007; Estrade et al., 2009; 60 Yang and Sturgeon, 2009; Sherman et al., 2010; Wiederhold et al., 2010; Ghosh et al., 2013; Smith et al., 2015; Janssen et al., 2016), but large extents of odd-MIF mainly occurred during photochemical reactions including photoreduction (Bergquist and Blum, 2007; Zheng and Hintelmann, 2009; Sherman et al., 2010; Zheng and Hintelmann, 2010b; Rose et al., 2015),



photodemethylation (Bergquist and Blum, 2007; Rose et al., 2015) and photooxidation (Sun et 65 al., 2016). Smaller but measureable degrees of odd-MIF were also reported for nonphotochemical abiotic reduction (Zheng and Hintelmann, 2010a) and evaporation of Hg^0 (Estrade et al., 2009; Ghosh et al., 2013). Interestingly, the results of laboratory and field investigations suggest that specific $\Delta^{199}\text{Hg}/\Delta^{201}\text{Hg}$ ratios are associated with such transformation processes, with a ratio of about 1.0 for photoreduction of inorganic Hg^{2+} 70 (Bergquist and Blum, 2007; Zheng and Hintelmann, 2009; Sherman et al., 2010; Zheng and Hintelmann, 2010b; Rose et al., 2015), about 1.3 for photodemethylation and 1.6 for Hg^0 evaporation and photooxidation (Bergquist and Blum, 2007; Estrade et al., 2009; Zheng and Hintelmann, 2010a; Ghosh et al., 2013; Rose et al., 2015; Sun et al., 2016). Even-MIF of Hg 75 isotope signatures were observed mostly in wet deposition, but the mechanism producing such fractionation remains unknown (Chen et al., 2012; Cai and Chen, 2016).

Prior studies have shown relatively constant Hg isotope compositions for GEM and very large variations of Hg isotope ratios for dissolved Hg^{2+} in wet precipitation (Gratz et al., 2010; Chen et al., 2012; Rolison et al., 2013; Wang et al., 2015; Yuan et al., 2015). A few studies reported that the Hg isotope compositions of PBM also show large variations (Rolison et al., 80 2013; Das et al., 2016; Huang et al., 2016; Yu et al., 2016; Xu et al., 2017). Among these limited studies, Rolison et al. (2013) reported $\delta^{202}\text{Hg}$ ($-1.61\text{\textperthousand}$ to $-0.12\text{\textperthousand}$) and $\Delta^{199}\text{Hg}$ values ($0.36\text{\textperthousand}$ to $1.36\text{\textperthousand}$) for Hg bound on total suspended particulates (TSP), with $\Delta^{199}\text{Hg}/\Delta^{201}\text{Hg}$ ratios of approximately unity, a value typical of photoreduction of inorganic Hg^{2+} . Das et al. (2016) found values of $\Delta^{199}\text{Hg}$ varied between $-0.31\text{\textperthousand}$ and $0.33\text{\textperthousand}$ for PM_{10} from Kolkata, eastern 85 India. It was suggested that PBM with longer residence times may have undergone greater photoreduction and hence exhibited more positive MIF. Huang et al. (2016) investigated Hg isotope compositions for $\text{PM}_{2.5}$ samples taken from Beijing, China, and attributed their observed seasonal variations in both MDF ($\delta^{202}\text{Hg}$ from $-2.18\text{\textperthousand}$ to $0.51\text{\textperthousand}$) and MIF ($\Delta^{199}\text{Hg}$



from $-0.53\text{\textperthousand}$ to $0.57\text{\textperthousand}$) to varied contributions from multiple sources of $\text{PM}_{2.5}\text{-Hg}$, while the
90 more positive $\Delta^{199}\text{Hg}$ values were likely produced by extensive photochemical reduction during long-range-transported. These prior results show that the Hg isotope approach can be employed for tracking sources and identifying possible transformation processes for airborne PM-Hg, and that PBM may undergo photochemical reactions that obscure its initial isotopic signature.

The goal of this study was to quantify short-term (diel) variations in the isotope composition
95 of $\text{PM}_{2.5}\text{-Hg}$ in an effort to elucidate if photochemical processes could impact overall contents and isotope compositions of PM-bound Hg in an urban environment. Unlike prior studies in which PM samples were collected continuously over 24 hrs or longer, we collected two $\text{PM}_{2.5}$ samples per 24 hrs with a daytime (D) sample between 8:00 a.m. and 6:30 p.m. and a nighttime (N) sample between 7:00 p.m. and 7:30 a.m.. It is intuitive that, while both D and N $\text{PM}_{2.5}$
100 samples may have similar local or regional sources if the wind trajectory remains unchanged, D samples could have been exposed to more solar radiation than N samples, likely resulting in diel variations in the Hg isotope compositions that are indicative of differences in photochemical transformation of $\text{PM}_{2.5}\text{-Hg}$. The specific objectives of this study were to verify and quantify whether Hg isotope compositions of $\text{PM}_{2.5}$ exhibit diel variations, and to elucidate
105 whether photochemical transformation is the dominant process for such diel variations.

2 Experimental section

2.1 Field site, sampling method, and preconcentration of $\text{PM}_{2.5}\text{-Hg}$

Beijing was selected as the area of study because of its well-known air pollution issue (Zhang
110 et al., 2007). Detailed information on the study site and $\text{PM}_{2.5}$ sampling procedures were given elsewhere (Huang et al., 2016). During the sampling period between Sept. 15th and Oct. 16th, 2015, the average outdoor temperatures were $22.1 \pm 3.0^\circ\text{C}$ and $18.5 \pm 2.7^\circ\text{C}$, and the average relative humidity were $45 \pm 20\%$ and $59 \pm 19\%$, for D and N, respectively. The $\text{PM}_{2.5}$ samples



were collected using a Tisch Environmental PM_{2.5} high volume air sampler, which collects
115 particles at a flow rate of 1.0 m³ min⁻¹ through a PM_{2.5} size selective inlet on a pre-combusted
(450°C for 6 hrs) quartz fiber filter (Pallflex 2500 QAT-UP, 20 cm × 25 cm, Pallflex Product
Co., USA). Quartz fiber filters were widely used to collect operationally defined PBM
(Schleicher et al., 2015; Zhang et al., 2015; Xu et al., 2017). A total of 61 samples including 30
D samples and 31 N samples were collected between 8:00 a.m. and 6:30 p.m. and 7:00 p.m. to
120 7:30 a.m., respectively, along with 2 field blanks. They were wrapped with aluminum film,
packed in plastic bags, and stored at -20°C in the lab prior to analysis. Meteorological data,
including temperature (T), relative humidity (RH), sunshine duration, daily average wind speed
(WS), were acquired from China Meteorological Administration (<http://data.cma.cn>), and the
atmospheric ozone content (P_{O_3}) was measured concurrently. These data are summarized in
125 Table S1.

2.2 Hg content and stable isotope measurements

The mass of each PM_{2.5} sample was gravimetrically quantified. Hg bound on each PM_{2.5} sample
was extracted and concentrated for analysis of Hg content and stable Hg isotopes using the
method reported previously (Huang et al., 2015). The details of the procedures are also given
130 in supplementary material (SI).

Among the 61 PM_{2.5} samples, 56 (including 26 D- and 30 N-samples) had sufficient Hg mass
(> 10 ng) and were further analyzed for Hg isotope compositions using a multicollector
inductively coupled plasma mass spectrometer (MC-ICP-MS, Nu Instruments Ltd., UK)
equipped with a continuous flow cold vapor generation system. Detailed protocols for the Hg
135 isotope analysis can be found in Huang et al. (2015) and also in SI. ^{196}Hg and ^{204}Hg were not
measured due to their very low abundance. Instrumental mass bias was corrected using an
internal standard (NIST SRM 997 Tl) and strict sample-standard bracketing with NIST SRM



3133 Hg standard. Delta (δ) notation is used to represent MDF in units of per mil (‰) as defined by the following equation (Blum and Bergquist, 2007):

140
$$\delta^x\text{Hg} (\text{\textperthousand}) = [({}^x\text{Hg}/{}^{198}\text{Hg})_{\text{sample}}/({}^x\text{Hg}/{}^{198}\text{Hg})_{\text{NIST3133}} - 1] \times 1000 \quad (1)$$

where $x = 199, 200, 201$, and 202 . MIF is reported as the deviation of a measured delta value from the theoretically predicted MDF value according to the equation:

$$\Delta^x\text{Hg} (\text{\textperthousand}) = \delta^x\text{Hg} - \beta \times \delta^{202}\text{Hg} \quad (2)$$

where the mass-dependent scaling factor β is $0.252, 0.5024$, and 0.752 for ${}^{199}\text{Hg}$, ${}^{200}\text{Hg}$ and ${}^{201}\text{Hg}$, respectively (Blum and Bergquist, 2007).

For quality assurance and control, we used NIST SRM 3177 Hg as a secondary standard and analyzed repeatedly during sample analysis session. The collective measurements of the NIST 3177 standard yielded average $\delta^{202}\text{Hg}$, $\Delta^{199}\text{Hg}$, $\Delta^{200}\text{Hg}$ and $\Delta^{201}\text{Hg}$ values of $-0.53\text{\textperthousand} \pm 0.09\text{\textperthousand}$, $-0.01\text{\textperthousand} \pm 0.04\text{\textperthousand}$, $0.00\text{\textperthousand} \pm 0.04\text{\textperthousand}$ and $-0.01\text{\textperthousand} \pm 0.07\text{\textperthousand}$ (2SD, $n = 17$). We also analyzed 150 regularly a well-known reference material UM-Almaden and a certified reference material (CRM) GBW07405, and the results showed average $\delta^{202}\text{Hg}$, $\Delta^{199}\text{Hg}$, $\Delta^{200}\text{Hg}$ and $\Delta^{201}\text{Hg}$ values of $-0.60\text{\textperthousand} \pm 0.09\text{\textperthousand}$, $-0.01\text{\textperthousand} \pm 0.04\text{\textperthousand}$, $0.01\text{\textperthousand} \pm 0.04\text{\textperthousand}$ and $-0.03\text{\textperthousand} \pm 0.07\text{\textperthousand}$ (2SD, $n = 17$) and of $-1.77\text{\textperthousand} \pm 0.14\text{\textperthousand}$, $-0.29\text{\textperthousand} \pm 0.06\text{\textperthousand}$, $0.00\text{\textperthousand} \pm 0.04\text{\textperthousand}$ and $-0.32\text{\textperthousand} \pm 0.07\text{\textperthousand}$ (2SD, $n = 6$), respectively. These values were consistent with previous results (Blum and Bergquist, 2007; Chen et al., 2010; Huang et al., 2015; Huang et al., 2016). The uncertainties of $\text{PM}_{2.5}$ -Hg isotope ratios listed in Table S2 were calculated based on repetitive measurements. However, if uncertainty of the isotopic compositions for a given sample was smaller than the uncertainty of CRM GBW07405, the uncertainty associated with that sample was assigned 2SD uncertainties (0.14‰, 0.06‰, 0.04‰ and 0.07‰ for $\delta^{202}\text{Hg}$, $\Delta^{199}\text{Hg}$, $\Delta^{200}\text{Hg}$ and $\Delta^{201}\text{Hg}$) obtained for long-160 term measurement of the CRM GBW07405.

2.3 Air mass backward trajectories



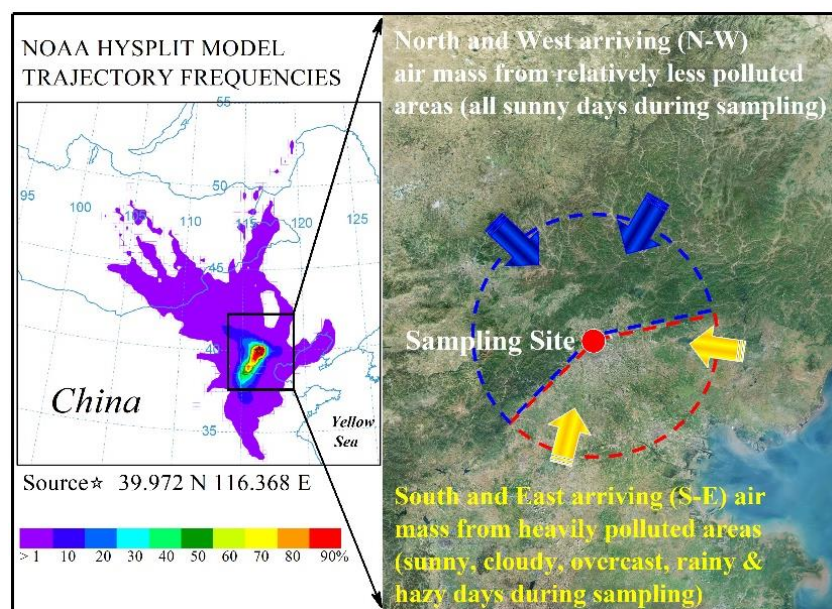
To identify possible pathways of PM_{2.5}-Hg transport, backward HYSPLIT trajectories of air masses at a height of 500 m above ground level and arriving at the sampling site were simulated.

Backward trajectories for each D or N sample were calculated every 1 hrs using the Internet-

165 Based HYSPLIT Trajectory Model and gridded meteorological data (Global Data Assimilation System, GDAS1) from the U.S. National Oceanic and Atmospheric Administration (NOAA)

(Fig. S1). The obtained average directions of arriving air masses for each sample were summarized in Table S1. The frequencies of backward trajectories were calculated for all the samples taken during Sept. 15th to Oct. 16th 2015 using the Internet-Based HYSPLIT Trajectory

170 Model and the archived GDAS0p5, with an interval of 3 hrs. Each trajectory had a total run time of 24 hrs and a grid resolution of 0.5 × 0.5 degree trajectory frequency. The simulation results showed the dominant air mass was arriving from southwest of the sampling site during the sampling period (see Fig. 1).



175 **Figure 1.** Geographic location of the PM_{2.5} collection site in Beijing, China (Baidu Map image) and average air mass back trajectories during sampling from Sept. 15th to Oct. 16th, 2015 (left), and characteristics of North-West vs. South-East arriving air masses.



2.4 Statistical analysis

T-test was performed for uncertainty analysis using IBM SPSS Statistics Version 22. Both
180 Paired Samples T-test and Independent Samples T-test were performed for diel variations of
Hg content, $\delta^{202}\text{Hg}$, $\Delta^{199}\text{Hg}$ and $\Delta^{200}\text{Hg}$, and their results were summarized in Table S3.

3 Results and discussion

3.1 Diel variation of PM_{2.5}-Hg

185 The chronological sequence of Hg stable isotope ratios, along with PM_{2.5} sample properties and
weather conditions for the 56 PM_{2.5} samples are presented in Figure 2 (see also Tables S1 and
S2 for quantitative atmospheric data and $\Delta^{201}\text{Hg}$ values). The major features of this dataset
include: i) large variations in both MDF and odd-MIF of Hg isotopes, ii) significant diel
differences in Hg isotope ratios, iii) correlations of weather conditions and air mass backward
190 trajectories with Hg isotope signals, and iv) detectable even-MIF.

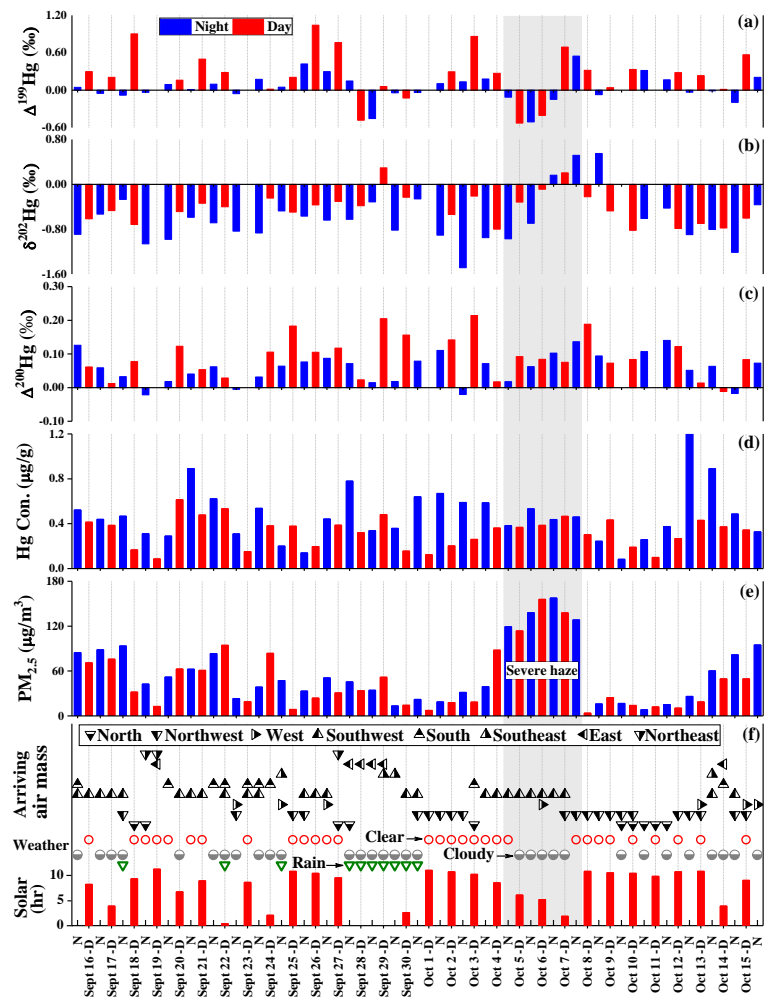


Figure 2. Chronological sequence of MIF ($\Delta^{199}\text{Hg}$ and $\Delta^{200}\text{Hg}$), MDF ($\delta^{202}\text{Hg}$), PM_{2.5}-Hg contents (C_{Hg}), and PM_{2.5} concentrations of the 56 samples collected during the daytime (D, red) and nighttime (N, blue), along with selected weather data including cumulative hours of sunshine (Solar) and air mass backward-trajectory directions.

The volumetric PM_{2.5} concentrations ranged from 4 to 158 $\mu\text{g m}^{-3}$ with an average value of $52 \pm 40 \mu\text{g m}^{-3}$ (1SD, $n = 61$) and the highest values ($> 100 \mu\text{g m}^{-3}$) detected during a severe haze event of Oct. 4th-7th. The mass-based Hg contents ranged from 0.08 to 1.22 $\mu\text{g g}^{-1}$ with a mean value of $0.40 \pm 0.21 \mu\text{g g}^{-1}$ (1SD, $n = 61$).



Hg isotope analysis showed that $\delta^{202}\text{Hg}$ values varied from $-1.49\text{\textperthousand}$ to $0.55\text{\textperthousand}$ (mean = $-0.53\text{\textperthousand}$ $\pm 0.40\text{\textperthousand}$, 1SD, $n = 56$), with the lowest value found in sample Oct-2-N and the highest in Oct-8-N. Significant odd-MIF of Hg isotopes was found and the $\Delta^{199}\text{Hg}$ values ranged from $-0.53\text{\textperthousand}$ to $1.04\text{\textperthousand}$ (mean = $0.14\text{\textperthousand} \pm 0.33\text{\textperthousand}$) with the lowest ($-0.53\text{\textperthousand}$) $\Delta^{199}\text{Hg}$ value on Oct-5-D during 205 the severe haze event and the highest ($1.04\text{\textperthousand}$) $\Delta^{199}\text{Hg}$ value on Sept-26-D during a sunny day (without cloud) (Fig. 2). All samples also displayed slight even-MIF, with $\Delta^{200}\text{Hg}$ values ranging from $-0.02\text{\textperthousand}$ to $0.21\text{\textperthousand}$ (average $0.07\text{\textperthousand} \pm 0.06\text{\textperthousand}$, 1SD, $n = 56$), which were significant compared to the detection precision of $\pm 0.04\text{\textperthousand}$. The overall variations of Hg isotope ratios for these 12-hr D/N PM_{2.5} samples are generally consistent with several prior reports for the 24-hr 210 PBM samples (Rolison et al., 2013; Das et al., 2016; Huang et al., 2016).

T-test results (Table S3) showed that diel variation was statistically significant ($p < 0.05$) for Hg contents, $\Delta^{199}\text{Hg}$, and $\Delta^{200}\text{Hg}$ values, as Hg contents for D-samples ($0.32 \pm 0.14 \text{ }\mu\text{g g}^{-1}$) were lower than N-samples ($0.48 \pm 0.24 \text{ }\mu\text{g g}^{-1}$), and $\Delta^{199}\text{Hg}$ and $\Delta^{200}\text{Hg}$ values for D-samples (mean of $0.26\text{\textperthousand} \pm 0.40\text{\textperthousand}$ and $0.09\text{\textperthousand} \pm 0.06\text{\textperthousand}$, respectively) were higher than N-samples 215 ($-0.04\text{\textperthousand} \pm 0.22\text{\textperthousand}$ and $0.06\text{\textperthousand} \pm 0.05\text{\textperthousand}$, respectively). However, PM_{2.5} concentrations and $\delta^{202}\text{Hg}$ had statistically insignificant ($p > 0.05$) diel variation.

3.2 Diel variation in odd-MIF of PM_{2.5}-Hg independent of air mass source

Many consecutive D-N sampling intervals had similar air mass back trajectories (Table S1 and 220 Fig. S1), suggesting that the dominant sources of PM_{2.5}-Hg did not vary over each such 24 hr sampling period. For example, pairs Sept-16-D and Sept-16-N, Sept-17-D and Sept-17-N, Sept-20-D and Sept-20-N, Sept-21-D and Sept-21-N, Oct-1-D and Oct-1-N, Oct-2-D and Oct-2-N, Oct-4-D and Oct-4-N have similar air mass trajectories from the southwest, and pairs Oct-8-D and Oct-8-N, Oct-9-D and Oct-9-N, Oct-10-D and Oct-10-N, Oct-11-D and Oct-11-N, Oct-12-225 D and Oct-12-N have similar air mass trajectories from the northwest and north (Fig. S1). It is



reasonable to assume, therefore, that each of these D-N PM_{2.5} sample pairs had identical dominant sources of PM_{2.5}-Hg and to expect that they would have very similar Hg isotope compositions. Instead, however, the data presented in Table S2 and Figure 2 revealed a unique and consistent pattern of diel variation in Hg isotope ratios; specifically, each PM_{2.5} D-sample
230 had a statistically significantly higher positive $\Delta^{199}\text{Hg}$ value (up to +1.04‰) than its consecutive PM_{2.5} N-sample.

The more positive $\Delta^{199}\text{Hg}$ values measured for the PM_{2.5} D-samples are highly unlikely uncharacteristic of known emission sources of PM_{2.5}-Hg. It is possible that PM_{2.5}-Hg from different emission sources may have different Hg isotope compositions. However, prior studies
235 showed that $\Delta^{199}\text{Hg}$ values of the PBM from dominant anthropogenic emission sources are generally negative or close to zero. Schleicher et al. (2015) demonstrated that coal combustion is likely the major source of PM_{2.5}-Hg in Beijing. Huang et al (2016) reported that regional anthropogenic activities such as coal combustion ($\Delta^{199}\text{Hg}$ values from -0.30‰ to 0.05‰), metal smelting (-0.20‰ to -0.05‰) and cement production (-0.25‰ to 0.05‰), as well as
240 biomass burning (low to -0.53‰) were likely the dominant sources of PM_{2.5}-Hg at this study site. As shown in Figure 2 and Table S1, the PM_{2.5} D-samples with high $\Delta^{199}\text{Hg}$ values (> 0.60‰) each had very different air mass back trajectories (Fig. S1). For instance, Sept-18-D (with $\Delta^{199}\text{Hg}$ value +0.90‰), Sept-26-D (with $\Delta^{199}\text{Hg}$ value +1.04‰) and Oct-3-D (with $\Delta^{199}\text{Hg}$ value +0.86‰) were associated with north, southwest, and north-south mixed air
245 masses, respectively. A reasonable explanation of these observations is that high positive $\Delta^{199}\text{Hg}$ values measured for D-samples resulted from PM_{2.5}-Hg transformation, specifically photoreduction, during atmospheric transport. Indeed, the diel variation of $\Delta^{199}\text{Hg}$ for PM_{2.5} D-N sample pairs may well reflect strong (D) versus less or no (N) influences of photochemical reactions under time-variant local and regional weather conditions.

250 **3.3 Photochemical reduction as a cause of odd-MIF in subset of daytime PM_{2.5} samples**

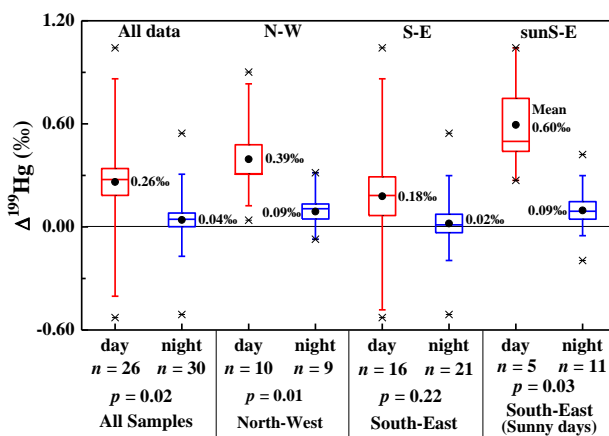


To detail the effects of photochemical reactions on the variation of Hg isotope ratios for PM_{2.5}-Hg, we regrouped our dataset into subsets corresponding to day and night. We further regrouped our results into two source-related subsets, south-east (S-E) and north-west (N-W), according to the air mass backward trajectories during each sampling event (Fig. 1), and two other subsets 255 corresponding to sunny days within the S-E group (sunS-E) and all sunny days (Sun), which includes sunS-E and N-W as N-W consisted entirely of sunny days. The N-W subset of PM_{2.5} was associated with an air mass that tracked from the north, northeast, northwest and west, relatively less polluted areas, and is therefore representative of long-range transport and relatively constant sources of PM_{2.5} and Hg (Huang et al., 2016). The S-E subset was associated 260 with an air mass that tracked from the south, southwest, southeast and east, heavily polluted and highly populated areas, and was characterized by relatively high contents of PM_{2.5}, likely from industrial sources in the region (coal fired power plants, coking and steel industries). Unlike the N-W arriving air mass which corresponded to all sunny days during the entire sampling period, the S-E arriving air mass was associated with a range of weather conditions 265 including hazy, cloudy, rainy, and sunny days. According to our results (Table S2 and Fig. 2), PM_{2.5} concentrations of the N-W subset ($23 \pm 19 \mu\text{g m}^{-3}$) were significantly ($p < 0.05$) lower than the S-E subset ($69 \pm 40 \mu\text{g m}^{-3}$), which is consistent with the fact that the N-W areas of Beijing were less industrialized, less populated and less polluted than the S-E areas. However, regardless of whether their associated air masses originated from moderately or heavily polluted 270 areas, both N-W and S-E subset samples showed diel variations in their Hg contents and isotope ratios (see Fig. 3 and discussion below). This, as discussed above, indicates that air mass source was not a dominant factor producing the diel variation of Hg isotope ratios in consecutive D-N PM_{2.5} samples.

The observed diel difference in $\Delta^{199}\text{Hg}$ values of PM_{2.5}-Hg is even more prominent and 275 statistically robust within subsets of PM_{2.5} samples regrouped according to their air mass



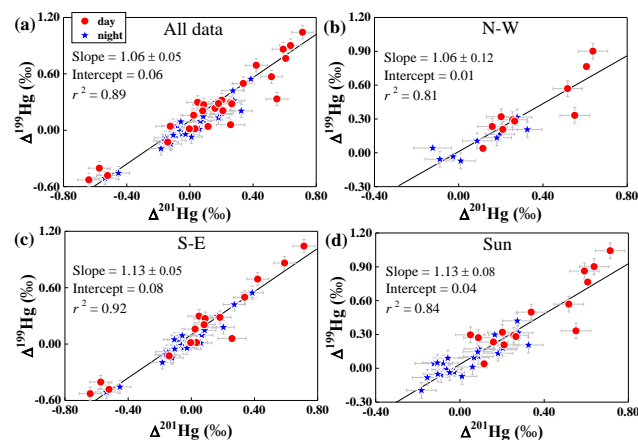
trajectories (i.e., PM_{2.5} source related) and sunny days (with greater extent of photochemical reactions). As shown in Figure 3, $\Delta^{199}\text{Hg}$ values for N-W subset samples collected during the day had a higher range (0.04‰ to 0.90‰) and mean ($0.39\text{‰} \pm 0.27\text{‰}$ SD, $n = 10$) compared to those (-0.07‰ to 0.32‰ , mean $= 0.09\text{‰} \pm 0.13\text{‰}$ SD, $n = 9$) for N-samples ($p = 0.02$).
280 Similarly, analysis of the sunS-E subset revealed a significant difference in $\Delta^{199}\text{Hg}$ values ($p = 0.03$) between sunny days and nights, but not when the entire S-E sample set ($p = 0.22$), which includes hazy, raining, and cloudy days, was considered. Since the N-W subset was associated with less polluted areas and the S-E subset was associated with heavily polluted and highly populated areas, the observation of significant diel variation of $\Delta^{199}\text{Hg}$ in PM_{2.5}-Hg within each
285 subset (Fig. 3) is consistent with the above conclusion that such variation of PM_{2.5}-Hg isotope ratios was not controlled by variation of Hg emission sources. The highly positive $\Delta^{199}\text{Hg}$ values observed for daytime samples within the Sun subset (Fig. S2) further supports the conclusion that PM_{2.5}-Hg was strongly affected by photochemical reactions on sunny days.



290 **Figure 3.** Diel variations of $\Delta^{199}\text{Hg}$ for PM_{2.5}-Hg for the entire dataset, the N-W subset, the S-E subset, and the S-E sunny days only subset. Note that all days included in the N-W subset were sunny. Diel differences within each subset were examined using the Independent Samples T-Test.



295 Linear correlations of $\Delta^{199}\text{Hg}$ versus $\Delta^{201}\text{Hg}$ for all 56 PM_{2.5} samples (Fig. 4a) and three subsets, N-W (Fig. 4b), S-E (Fig. 4c), and Sun (Fig. 4d), yielded slopes of 1.06 ± 0.05 (1SD, $r^2 = 0.89$), 1.06 ± 0.12 ($r^2 = 0.81$), 1.13 ± 0.05 ($r^2 = 0.92$) and 1.13 ± 0.08 ($r^2 = 0.84$), respectively (Fig. 4). Such slopes are all indicative of photochemical reduction of Hg²⁺ according to prior studies (Bergquist and Blum, 2007; Zheng and Hintelmann, 2009). The photoreduction process 300 is further evidenced by a progressive increase in $\Delta^{199}\text{Hg}$ from zero or slightly negative values to positive values as the content of Hg in PM_{2.5} (C_{Hg}) decreased in D-samples (Fig. S1a). This trend is statistically more significant ($p < 0.05$) for D-samples within the N-W and Sun subsets (Figs. S1-b and -d). Similarly, for all sunny day samples, a positive correlation ($p < 0.05$) was 305 also observed between $\Delta^{199}\text{Hg}$ and $\delta^{202}\text{Hg}$ (Fig. S3), consistent with prior experimental results (Bergquist and Blum, 2007; Zheng and Hintelmann, 2009). Collectively, the Hg isotope results suggest that photochemical reduction is an important process during the transport of PM_{2.5}-Hg in the atmosphere.



310 **Figure 4.** Correlations between $\Delta^{199}\text{Hg}$ and $\Delta^{201}\text{Hg}$ for different subsets of PM_{2.5} samples: a) all data, b) North-West (N-W), c) South-East (S-E) and d) All sunny days (Sun). The slope, intercept and r^2 of the line from simple linear regression. Vertical and horizontal error bars correspond to 2SD analytical precision.



Among all D-samples, $\Delta^{199}\text{Hg}$ is only weakly correlated with sunshine duration ($r^2 = 0.20, p = 0.02$). However, $\Delta^{199}\text{Hg}$ values for all D-samples collected on days with sunshine durations >8 hrs are positive whereas half of the $\Delta^{199}\text{Hg}$ values for samples collected on cloudy or hazy days with shorter sunshine durations are negative or near zero (Fig. S4). In addition, a significant positive linear correlation between $\Delta^{199}\text{Hg}$ values and atmospheric ozone contents (P_{O_3}) ($r^2 = 0.517, p < 0.01$) for all but four daytime samples was obtained (Fig. S5). The four 315 outliners (Sept-16-D, Sept-17-D, Oct-5-D and Oct-6-D) were collected on days with high ozone (P_{O_3} above 50 ppbv) and severe smog formation. Conversely, no significant correlation ($p > 0.05$) between $\Delta^{199}\text{Hg}$ and P_{O_3} was found for the nighttime samples.

The increase in $\Delta^{199}\text{Hg}$ of daytime PM_{2.5}-Hg with sunlight duration and ozone concentration indicates that the physical and photochemical conditions of the atmosphere may affect the 325 atmospheric transformation of PM_{2.5}-Hg. A prior experimental study showed that GEM oxidation can produce negative $\Delta^{199}\text{Hg}$ values in oxidized Hg²⁺ with $\Delta^{199}\text{Hg}/\Delta^{201}\text{Hg}$ ratios of 1.6 and 1.9 for Br and Cl radical initiated oxidations (Sun et al., 2016). We can exclude the possible contribution of Hg⁰ oxidation to PM_{2.5}-Hg, given the fact that $\Delta^{199}\text{Hg}/\Delta^{201}\text{Hg}$ ratio was about 1.1 and most PM_{2.5}-Hg samples collected during the daytime when Br and Cl radicals 330 could form had positive $\Delta^{199}\text{Hg}$ values. Thus it is highly unlikely that oxidation would have caused the diel variation in Hg isotopes in PM_{2.5}. However, the exception to the observed relationships between $\Delta^{199}\text{Hg}$ with sunlight duration, and ozone concentration show that in a highly oxidizing atmosphere (higher P_{O_3}) such as occurs during extreme smog events, the odd-MIF of Hg isotopes in PM_{2.5} may decrease or reverse. A possible explanation for this effect 335 may be the increased production of GOM and its collection with PM_{2.5}-Hg during such smog events. While PM_{2.5}-Hg samples collected on quartz fiber filters may include some GOM (Lynam and Keeler, 2002), this contribution was likely small in most of our D and N samples due to the opposing diel trends in the concentrations of PBM and GOM in urban air (Engle et



al., 2010). GOM would therefore not have had a major effect on the observed diel variations of
340 $\Delta^{199}\text{Hg}$ values for $\text{PM}_{2.5}\text{-Hg}$ and may have in fact masked an even larger MIF signature due to
the photoreduction of PBM during the day.

Interestingly, negative $\Delta^{199}\text{Hg}$ values in daytime $\text{PM}_{2.5}\text{-Hg}$ were only observed during a rainy
day and an extreme smog event. Scavenging of locally produced GOM during rain or smog
events may therefore have contributed to the reversal of the odd-MIF signature of Hg collected
345 as $\text{PM}_{2.5}$ at these times. In addition, the negative $\Delta^{199}\text{Hg}$ values in $\text{PM}_{2.5}$ may have resulted from
the contribution of biomass burning with limited photoreduction effect during period of less
sunshine (Fig. 2 and Table S1) since plant foliage has negative $\Delta^{199}\text{Hg}$ values (Yu et al., 2016)
and more negative $\Delta^{199}\text{Hg}$ values (down to $-0.53\text{\textperthousand}$) of $\text{PM}_{2.5}\text{-Hg}$ in Beijing were related to
biomass burning, a source of $\text{PM}_{2.5}\text{-Hg}$ south of Beijing in autumn (Huang et al., 2016). This
350 could further explain the relatively lower $\Delta^{199}\text{Hg}$ values in the majority of the N-samples (for
example, Sept-28-N and Oct-5-N with $\Delta^{199}\text{Hg}$ of $-0.46\text{\textperthousand}$ and $-0.51\text{\textperthousand}$), even in those collected
under clear weathering condition. Indeed, each bulk sample collected during night time was a
mixture of the leftover $\text{PM}_{2.5}$ (with positive odd-MIF) from the previous daytime and the $\text{PM}_{2.5}$
355 newly input from various sources including industrial emissions (with close to zero $\Delta^{199}\text{Hg}$)
and biomass burning (somewhat negative $\Delta^{199}\text{Hg}$) (Huang et al., 2016) during nighttime.

While our results cannot exclude the effects of other possible processes, such as oxidation,
adsorption (and desorption), and precipitation, based on the limited previous studies (Jiskra et
al., 2012; Smith et al., 2015; Sun et al., 2016), these processes are not likely to be important to
the diel variation of odd-MIF of Hg isotopes in $\text{PM}_{2.5}\text{-Hg}$ we observed.

360

3.4 Photochemical reduction as a cause of diel variation in odd-MIF in day-night sample pairs of $\text{PM}_{2.5}$



To explore the possible causes of diel variation in odd-MIF of Beijing PM_{2.5}-Hg further, we examined four subgroups of PM_{2.5} samples, each of which included 2 to 4 consecutive pairs of 365 D-N samples that were collected during time periods of relatively constant atmospheric conditions (i.e., not being hazy, rainy or windy or having extremely high ozone (P_{O_3} above 50 ppbv)). Within each of the four subgroups, $\Delta^{199}\text{Hg}$ and $\delta^{202}\text{Hg}$ values were lower at night than during the previous or following day (Figs. 5-a and -b). As shown in Figure 5c, there is a significant positive correlation ($p < 0.01$) between $\Delta^{199}\text{Hg}$ and $\delta^{202}\text{Hg}$ values for all samples in 370 these four subgroups, with average values for both day and night falling right on the best fit line. The slope of this line is 1.15 ± 0.33 , which is consistent with the reported value of 1.15 ± 0.07 for photochemical reduction of Hg²⁺ in aqueous solution (Bergquist and Blum, 2007). Coincidentally, the contents of Hg in PM_{2.5} (C_{Hg}) were higher in N-samples than in immediately preceding or following D-samples (Fig. 5d), indicating a negative linear relationship between 375 $\Delta^{199}\text{Hg}$ values and C_{Hg} (Fig. 5e). Moreover, eight of the total eleven daytime samples among the four subgroups showed a positive linear correlation between $\Delta^{199}\text{Hg}$ and the total cumulative daily solar radiation on a horizontal surface (SH) (Fig. 5f). These eleven samples also showed a negative correlation between the logarithmic values of C_{Hg} and SH (Fig. 5g). These correlations are consistent with the photochemical reduction of divalent Hg observed 380 under laboratory conditions, and thus strongly support the hypothesis that photochemical reduction is an important process controlling the fate of ambient atmospheric PM_{2.5}-Hg. Given its diel trend and relatively large range, the MIF of odd Hg isotopes in Beijing PM_{2.5} we observed was most likely due to the magnetic isotope effect (MIE), which has been invoked to explain MIF during the photochemical reduction of aqueous Hg²⁺ (Zheng and Hintelmann, 385 2010b).

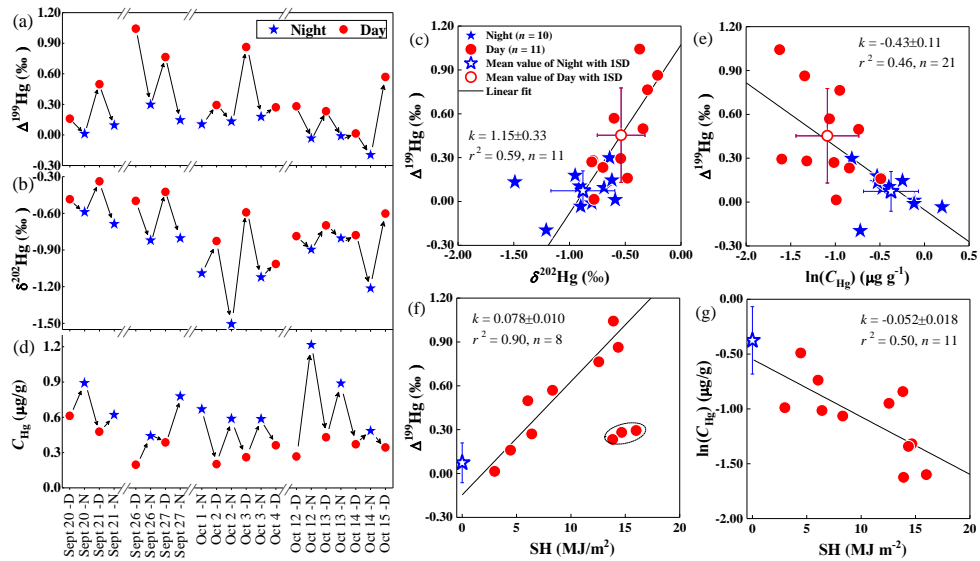


Figure 5. Hg isotope ratios and contents in four subgroups of consecutive pairs of day-night samples collected during periods of relatively constant atmospheric conditions. Linear correlations between $\Delta^{199}\text{Hg}$ and $\delta^{202}\text{Hg}$ (c), C_{Hg} (e) and the total cumulative daily solar radiation on a horizontal surface (SH , MJ m^{-2}) (f), and between C_{Hg} and SH (g) were displayed.

390

3.5 Even isotope MIF

Diel variation of $\Delta^{200}\text{Hg}$ signatures was also observed in $\text{PM}_{2.5}\text{-Hg}$. Prior studies reported mainly positive $\Delta^{200}\text{Hg}$ values for wet precipitation (up to $1.24\text{\textperthousand}$) (Gratz et al., 2010; Chen et al., 2012; Wang et al., 2015; Yuan et al., 2015) and aerosols ($-0.05\text{\textperthousand}$ to $0.28\text{\textperthousand}$) (Rolison et al., 2013; Das et al., 2016; Huang et al., 2016). Even Hg isotope MIF has been attributed to complex redox processes occurring in the upper atmosphere, but the underlying mechanisms remain unclear (Mead et al., 2013; Eiler et al., 2014). Thus, the even-MIF signatures may suggest a small proportion of $\text{PM}_{2.5}\text{-Hg}$ is likely originated from the upper atmosphere, through for example long-term transport. Given the fact that all samples displayed only slightly positive $\Delta^{200}\text{Hg}$ (average $0.07\text{\textperthousand} \pm 0.06\text{\textperthousand}$, 1SD), this contribution may be very limited. In addition, $\Delta^{200}\text{Hg}$ values are weakly, but significantly correlated with $\Delta^{199}\text{Hg}$ ($r^2 = 0.13$, $p < 0.01$) (Fig.

395

400



S6) and $\delta^{202}\text{Hg}$ ($r^2 = 0.27$, $p < 0.01$) (Fig. S7). No mechanistic explanation is available yet for such observations, however.

405

4 Conclusions

This study showed significant diel variations of Hg isotopic compositions for ambient $\text{PM}_{2.5}$ -Hg collected in the city of Beijing. The Hg isotope signatures featured a large range of MDF ($\delta^{202}\text{Hg}$ value from $-1.49\text{\textperthousand}$ to $0.55\text{\textperthousand}$, mean of $-0.53\text{\textperthousand} \pm 0.40\text{\textperthousand}$) and significant ($p < 0.05$)
410 MIF with more positive $\Delta^{199}\text{Hg}$ values in daytime samples ($0.26\text{\textperthousand} \pm 0.40\text{\textperthousand}$) than at night ($0.04\text{\textperthousand} \pm 0.22\text{\textperthousand}$). The results clearly indicated that the Hg isotope compositions of $\text{PM}_{2.5}$ -Hg are impacted variously by both weather conditions (such as sunlight duration), which may promote the photochemical reaction, and directions of air mass trajectories, which are related to possible sources of $\text{PM}_{2.5}$. D-N paired samples having similar air mass backward trajectories and hence
415 similar sources exhibited strong positive correlations between $\Delta^{199}\text{Hg}$ and $\Delta^{201}\text{Hg}$ with a slope of 1.1 and $\Delta^{199}\text{Hg}$ and $\delta^{202}\text{Hg}$ with a slope of 1.15, and a decrease in the content of Hg in $\text{PM}_{2.5}$ as $\Delta^{199}\text{Hg}$ increased. These results provide isotopic evidence that local, daytime photochemical reduction of divalent Hg is of critical importance to the fate of $\text{PM}_{2.5}$ -Hg in urban atmosphere. Although the specific reactions and mechanisms that control Hg isotope fractionation (MDF
420 and MIF) in Beijing $\text{PM}_{2.5}$ could not be explicitly determined from this field study, our result illustrated that, in addition to variation in sources, photochemical reduction appears to be an important process that affects both the content and isotopic composition of $\text{PM}_{2.5}$ -Hg. Further systematic study is thus needed to better quantify the photoreduction of $\text{PM}_{2.5}$ -Hg to estimate the percentage of reduced Hg it produces and its impact on the global biogeochemical cycling
425 of Hg.



Acknowledgments. This study was supported financially by the National Key Research and Development Program of China (No. 2017YFC0212702), Natural Science Foundation of China (no. 41701268, 41625012, 41273023), Guizhou Scientific Research Program (No. 20161158) 430 and State Key Laboratory of Organic Geochemistry (OGL-201501).

References

Bergquist, B. A., and Blum, J. D.: Mass-dependent and -independent fractionation of Hg isotopes by photoreduction in aquatic systems, *Science*, 318, 417-420, 2007.

435 Blum, J. D., and Bergquist, B. A.: Reporting of variations in the natural isotopic composition of mercury, *Anal. Bioanal. Chem.*, 388, 353-359, 2007.

Cai, H., and Chen, J.: Mass-independent fractionation of even mercury isotopes, *Science Bulletin*, 61, 116-124, 10.1007/s11434-015-0968-8, 2016.

Chen, J. B., Hintelmann, H., and Dimock, B.: Chromatographic pre-concentration of Hg from 440 dilute aqueous solutions for isotopic measurement by MC-ICP-MS, *J. Anal. At. Spectrom.*, 25, 1402-1409, 2010.

Chen, J. B., Hintelmann, H., Feng, X. B., and Dimock, B.: Unusual fractionation of both odd and even mercury isotopes in precipitation from Peterborough, ON, Canada, *Geochim. Cosmochim. Acta*, 90, 33-46, 2012.

445 Das, R., Wang, X., Khezri, B., Webster, R. D., Sikdar, P. K., and Datta, S.: Mercury isotopes of atmospheric particle bound mercury for source apportionment study in urban Kolkata, India, *Elementa: Science of the Anthropocene*, 4, 000098, 2016.

Eiler, J. M., Bergquist, B., Bourg, I., Cartigny, P., Farquhar, J., Gagnon, A., Guo, W., Halevy, I., Hofmann, A., Larson, T. E., Levin, N., Schauble, E. A., and Stolper, D.: Frontiers of stable 450 isotope geoscience, *Chem. Geol.*, 372, 119-143, 2014.

Engle, M. A., Tate, M. T., Krabbenhoft, D. P., Schauer, J. J., Kolker, A., Shanley, J. B., and Bothner, M. H.: Comparison of atmospheric mercury speciation and deposition at nine sites across central and eastern North America, *Journal of Geophysical Research: Atmospheres*, 115, 2010.



455 Estrade, N., Carignan, J., Sonke, J. E., and Donard, O. F. X.: Mercury isotope fractionation
during liquid-vapor evaporation experiments, *Geochim. Cosmochim. Acta*, 73, 2693-2711,
2009.

Ghosh, S., Schauble, E. A., Lacrampe Couloume, G., Blum, J. D., and Bergquist, B. A.:
Estimation of nuclear volume dependent fractionation of mercury isotopes in equilibrium
460 liquid-vapor evaporation experiments, *Chem. Geol.*, 336, 5-12, 2013.

Gratz, L. E., Keeler, G. J., Blum, J. D., and Sherman, L. S.: Isotopic composition and
fractionation of mercury in Great Lakes precipitation and ambient air, *Environ. Sci. Technol.*,
44, 7764-7770, 2010.

Hintelmann, H., and Lu, S. Y.: High precision isotope ratio measurements of mercury isotopes
465 in cinnabar ores using multi-collector inductively coupled plasma mass spectrometry,
Analyst, 128, 635-639, 2003.

Huang, Q., Liu, Y. L., Chen, J. B., Feng, X. B., Huang, W. L., Yuan, S. L., Cai, H. M., and Fu,
X. W.: An improved dual-stage protocol to pre-concentrate mercury from airborne particles
for precise isotopic measurement, *J. Anal. At. Spectrom.*, 30, 957-966, 2015.

470 Huang, Q., Chen, J., Huang, W., Fu, P., Guinot, B., Feng, X., Shang, L., Wang, Z., Wang, Z.,
Yuan, S., Cai, H., Wei, L., and Yu, B.: Isotopic composition for source identification of
mercury in atmospheric fine particles, *Atmos. Chem. Phys.*, 16, 11773-11786, 2016.

Jackson, T. A., Muir, D. C. G., and Vincent, W. F.: Historical variations in the stable isotope
composition of mercury in Arctic Lake sediments, *Environ. Sci. Technol.*, 38, 2813-2821,
475 2004.

Jackson, T. A., Whittle, D. M., Evans, M. S., and Muir, D. C. G.: Evidence for mass-
independent and mass-dependent fractionation of the stable isotopes of mercury by natural
processes in aquatic ecosystems, *Appl. Geochem.*, 23, 547-571, 2008.

Janssen, S. E., Schaefer, J. K., Barkay, T., and Reinfelder, J. R.: Fractionation of mercury stable
480 isotopes during microbial methylmercury production by iron- and sulfate-reducing bacteria,
Environ. Sci. Technol., 50, 8077-8083, 2016.

Jiskra, M., Wiederhold, J. G., Bourdon, B., and Kretzschmar, R.: Solution speciation controls
mercury isotope fractionation of Hg(II) sorption to goethite, *Environ. Sci. Technol.*, 46, 6654-
6662, 2012.



485 Kritee, K., Blum, J. D., Johnson, M. W., Bergquist, B. A., and Barkay, T.: Mercury stable isotope fractionation during reduction of Hg(II) to Hg(0) by mercury resistant microorganisms, *Environ. Sci. Technol.*, 41, 1889-1895, 2007.

Lynam, M. M., and Keeler, G. J.: Comparison of methods for particulate phase mercury analysis: Sampling and analysis, *Anal. Bioanal. Chem.*, 374, 1009-1014, 2002.

490 Mead, C., Lyons, J. R., Johnson, T. M., and Anbar, A. D.: Unique Hg stable isotope signatures of compact fluorescent lamp-sourced Hg, *Environ. Sci. Technol.*, 47, 2542-2547, 2013.

Rolison, J. M., Landing, W. M., Luke, W., Cohen, M., and Salters, V. J. M.: Isotopic composition of species-specific atmospheric Hg in a coastal environment, *Chem. Geol.*, 336, 37-49, 2013.

495 Rose, C. H., Ghosh, S., Blum, J. D., and Bergquist, B. A.: Effects of ultraviolet radiation on mercury isotope fractionation during photo-reduction for inorganic and organic mercury species, *Chem. Geol.*, 405, 102-111, 2015.

Schleicher, N. J., Schäfer, J., Blanc, G., Chen, Y., Chai, F., Cen, K., and Norra, S.: Atmospheric particulate mercury in the megacity Beijing: Spatio-temporal variations and source 500 apportionment, *Atmos. Environ.*, 109, 251-261, 2015.

Selin, N. E.: Global biogeochemical cycling of mercury: A review, *Annu. Rev. Env. Resour.*, 34, 43-63, 2009.

Sherman, L. S., Blum, J. D., Johnson, K. P., Keeler, G. J., Barres, J. A., and Douglas, T. A.: Mass-independent fractionation of mercury isotopes in Arctic snow driven by sunlight, 505 *Nature Geosci.*, 3, 173-177, 2010.

Sherman, L. S., Blum, J. D., Keeler, G. J., Demers, J. D., and Dvonch, J. T.: Investigation of local mercury deposition from a coal-fired power plant using mercury isotopes, *Environ. Sci. Technol.*, 46, 382-390, 2012.

Smith, R. S., Wiederhold, J. G., and Kretzschmar, R.: Mercury isotope fractionation during 510 precipitation of metacinnabar (β -HgS) and montroydite (HgO), *Environ. Sci. Technol.*, 49, 4325-4334, 2015.

Subir, M., Ariya, P. A., and Dastoor, A. P.: A review of the sources of uncertainties in atmospheric mercury modeling II. Mercury surface and heterogeneous chemistry—A missing link, *Atmos. Environ.*, 46, 1-10, 2012.



515 Sun, G., Sommar, J., Feng, X., Lin, C.-J., Ge, M., Wang, W., Yin, R., Fu, X., and Shang, L.: Mass-dependent and -independent fractionation of mercury isotope during gas-phase oxidation of elemental mercury vapor by atomic Cl and Br, *Environ. Sci. Technol.*, 50, 9232-9241, 2016.

520 Wang, Z., Chen, J., Feng, X., Hintelmann, H., Yuan, S., Cai, H., Huang, Q., Wang, S., and Wang, F.: Mass-dependent and mass-independent fractionation of mercury isotopes in precipitation from Guiyang, SW China, *C. R. Geosci.*, 347, 358-367, 2015.

Wiederhold, J. G., Cramer, C. J., Daniel, K., Infante, I., Bourdon, B., and Kretzschmar, R.: Equilibrium mercury isotope fractionation between dissolved Hg(II) species and thiol-bound Hg, *Environ. Sci. Technol.*, 44, 4191-4197, 2010.

525 Xu, H., Sonke, J. E., Guinot, B., Fu, X., Sun, R., Lanzanova, A., Candaup, F., Shen, Z., and Cao, J.: Seasonal and annual variations in atmospheric Hg and Pb isotopes in Xi'an, China, *Environ. Sci. Technol.*, 51, 3759-3766, 2017.

Yang, L., and Sturgeon, R.: Isotopic fractionation of mercury induced by reduction and ethylation, *Anal. Bioanal. Chem.*, 393, 377-385, 2009.

530 Yu, B., Fu, X., Yin, R., Zhang, H., Wang, X., Lin, C.-J., Wu, C., Zhang, Y., He, N., Fu, P., Wang, Z., Shang, L., Sommar, J., Sonke, J. E., Maurice, L., Guinot, B., and Feng, X.: Isotopic composition of atmospheric mercury in China: New evidence for sources and transformation processes in air and in vegetation, *Environ. Sci. Technol.*, 50, 9262-9269, 2016.

Yuan, S., Zhang, Y., Chen, J., Kang, S., Zhang, J., Feng, X., Cai, H., Wang, Z., Wang, Z., and 535 Huang, Q.: Large variation of mercury isotope composition during a single precipitation event at Lhasa city, Tibetan Plateau, China, *Procedia Earth and Planetary Science*, 13, 282-286, 2015.

Zhang, L., Wang, S. X., Wang, L., Wu, Y., Duan, L., Wu, Q. R., Wang, F. Y., Yang, M., Yang, H., Hao, J. M., and Liu, X.: Updated emission inventories for speciated atmospheric mercury from anthropogenic sources in China, *Environ. Sci. Technol.*, 49, 3185-3194, 2015.

540 Zhang, Q., Jimenez, J. L., Canagaratna, M. R., Allan, J. D., Coe, H., Ulbrich, I., Alfarra, M. R., Takami, A., Middlebrook, A. M., Sun, Y. L., Dzepina, K., Dunlea, E., Docherty, K., DeCarlo, P. F., Salcedo, D., Onasch, T., Jayne, J. T., Miyoshi, T., Shimono, A., Hatakeyama, S., Takegawa, N., Kondo, Y., Schneider, J., Drewnick, F., Borrmann, S., Weimer, S., Demerjian,



545 K., Williams, P., Bower, K., Bahreini, R., Cottrell, L., Griffin, R. J., Rautiainen, J., Sun, J.
Y., Zhang, Y. M., and Worsnop, D. R.: Ubiquity and dominance of oxygenated species in
organic aerosols in anthropogenically-influenced Northern Hemisphere midlatitudes,
Geophys. Res. Lett., 34, 2007.

550 Zheng, W., and Hintelmann, H.: Mercury isotope fractionation during photoreduction in natural
water is controlled by its Hg/DOC ratio, Geochim. Cosmochim. Acta, 73, 6704-6715, 2009.

Zheng, W., and Hintelmann, H.: Nuclear field shift effect in isotope fractionation of mercury
during abiotic reduction in the absence of light, J. Phys. Chem. A, 114, 4238-4245, 2010a.

555 Zheng, W., and Hintelmann, H.: Isotope fractionation of mercury during its photochemical
reduction by low-molecular-weight organic compounds, J. Phys. Chem. A, 114, 4246-4253,
2010b.